

Comprehensive understanding of H adsorption on MoO₃ from systematic *ab initio* simulations

Yuji Ikeda,^{1,*} Deven Estes,² and Blazej Grabowski¹

¹*Institute for Materials Science, University of Stuttgart, Pfaffenwaldring 55, 70569 Stuttgart, Germany*

²*Institute of Technical Chemistry, University of Stuttgart, Pfaffenwaldring 55, 70569, Stuttgart, Germany*

During many of its applications (especially as a catalyst support material), MoO₃ acts as a medium for hydrogen storage via hydrogen spillover (H atom donation from proton and electron sources to a support), for which the energetics of H atoms on MoO₃ are of importance. Despite the seeming simplicity of hydrogen spillover, previously reported *ab initio* results for the H adsorption on MoO₃ contradict both experimental work and other *ab initio* results. In the present study, we resolve these discrepancies and provide a comprehensive *ab initio* understanding of H adsorption for MoO₃ in the bulk and on the surface. To this end, we systematically investigate various exchange–correlation functionals and various H concentrations, and we carefully track the various relevant H positions. For a dilute H concentration, the asymmetric oxygen site (O_a) is found to be energetically the most favorable. With increasing H content, the difference of the H adsorption energies between the terminal (O_t) and the O_a sites becomes smaller. Previous contradictions are ascribed mostly to the disregard of the H position along the O_a–O_a zig-zag chains in the intrabilayer region. Using the modern non-empirical strongly-constrained and appropriately-normed (SCAN) meta-generalized gradient approximation (GGA), the dilute-limit H adsorption energies are obtained as -2.89 eV/(H atom) and -2.97 eV/(H atom) in the bulk and on the surface, respectively, and the activation energy of H diffusion between the O_a sites as 0.11 – 0.15 eV/(H atom), consistent with previous experiments.

1. INTRODUCTION

1.1. Motivation

The α phase of MoO₃ is a layered transition-metal oxide and a semiconductor with a wide band gap of 2.8 eV as a single crystal [1]. This oxide has a number of technologically important applications, e.g., as a cathode material in rechargeable lithium ion batteries [2, 3], as a catalyst [4–7], in photochromic and electrochromic devices [8, 9], in optoelectronic nanodevices [10], as a gas sensor [11, 12], and as a capacitive energy storage [13]. Among the various applications, MoO₃ is used as a support material for hydrogen storage [5] via the so-called hydrogen spillover mechanism [14, 15]. An unusually high hydrogen capacity can be achieved via the dissociative chemisorption of H atoms on a noble-metal catalyst and the subsequent migration of these H atoms onto the surface of a MoO₃ support material.

To understand the catalytic activity of α -MoO₃ as well as the hydrogen spillover onto it, the energetics of H atoms are of critical importance, and in particular it is essential to know the energetically favorable H adsorption sites on MoO₃. In experiments, these issues have been addressed by considering hydrogen bronze, i.e., H_{*x*}MoO₃ with $0 < x \leq 2$. For a relatively low H content of $x \leq 0.5$, powder neutron diffraction [16, 17] and nuclear magnetic resonance [18, 19] showed that H is bound to the asymmetric oxygen (O_a) sites and resides in the intrabilayer region. For higher H contents of $1.55 < x \leq 2$, pow-

der neutron diffraction [20, 21] showed that H is bound to the terminal oxygen (O_t) sites and resides in the interbilayer region. We can thus qualitatively expect that the H adsorption energy substantially depends on the O site as well as the H content. It is, however, very difficult to address this dependence quantitatively solely by experiments.

In principle, *ab initio* calculations can help to provide a detailed understanding of H spillover onto MoO₃. H adsorption in bulk α -MoO₃ was investigated in a few previous *ab initio* studies [22, 23]. H adsorption on the surface of α -MoO₃ was likewise addressed in several papers in relation to the surface reaction of various adsorbates such as the hydrogen atom itself [24], methyl radical [25, 26], ethylene [27], acetaldehyde [28] acetone [29, 30], methanol [31], and formaldehyde [31]. Most of these studies reported their computed H adsorption energies as well as the energetically favorable O sites for the H adsorption. These results are, however, contradictory among each other (cf. Section 1.4) and sometimes even with respect to the experimental findings mentioned above. These contradictions have not yet found any explanation, and this discrepancy has clearly impeded the establishment of reliable *ab initio* results.

In the present study, we systematically investigate H adsorption for α -MoO₃ in the bulk and on the surface based on *ab initio* simulations. We consider various H locations, even for the same O site (cf. Section 1.3), as well as the impact of the H content. We investigate various exchange–correlation functionals with and without consideration of the van der Waals (vdW) interaction. We offer a comprehensive understanding and resolve the contradictions among the previously reported *ab initio* results. Our results provide the basis for a better inter-

* yuji.ikeda@imw.uni-stuttgart.de

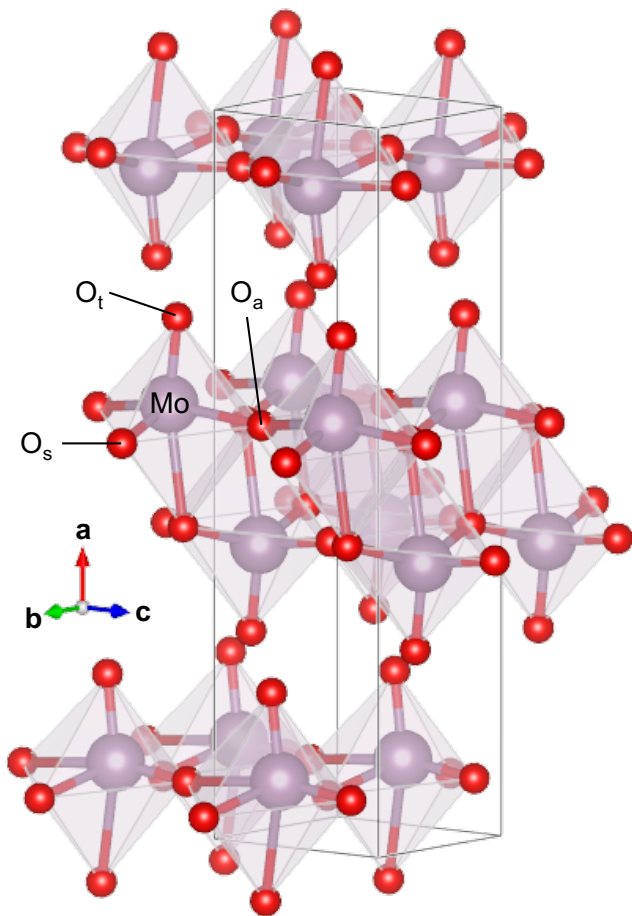


Figure 1. Crystal structure of α - MoO_3 . The purple and the red spheres represent Mo and O atoms, respectively. Visualization has been performed using VESTA [32].

pretation of experimental observations.

1.2. Crystal structure of α - MoO_3

The ground state of MoO_3 is called the α phase (Figure 1), and it is characterized by the space group $Pnma$ (No. 62) (or equivalently $Pbnm$ in the **cab** setting [33]). The structure consists of bilayers of edge-sharing MoO_6 octahedra, and the bilayers attract each other by the vdW interaction. There are three symmetrically inequivalent O sites in α - MoO_3 . The oxygen at the terminal site (O_t) is bound to only one Mo atom and faces the vdW gap. The oxygen at the assymmetric site (O_a) is bound to two Mo atoms with different Mo–O bond lengths. The oxygen at the symmetric site (O_s) is bound to three Mo atoms, among which two Mo–O bonds lie out of the reflection plane and are symmetrically equivalent. Mo as well as all the symmetrically inequivalent O atoms belong to distinct $4c$ Wyckoff positions.

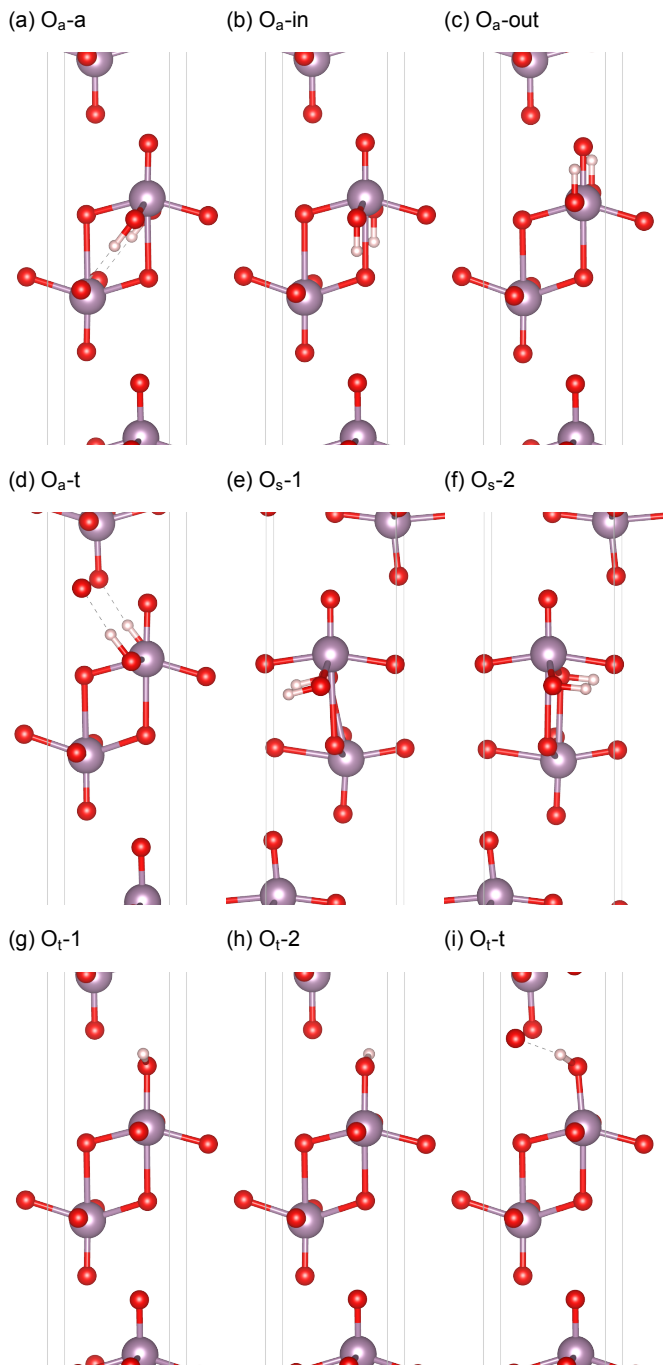


Figure 2. H adsorption sites in α - MoO_3 investigated in the present study. Here we show the optimized structures in bulk $\text{H}_{0.25}\text{MoO}_3$ using the SCAN functional.

1.3. H adsorption locations

An H atom may be adsorbed onto one of the three symmetrically inequivalent O sites in α - MoO_3 . Further, even for the same O site, H can sit at various locations, as exemplified in Figure 2. Specifically, for the O_a site, the H atom can be located on the O_a – O_a zig-zag chain in the intralayer region (see Figure 3), a location we

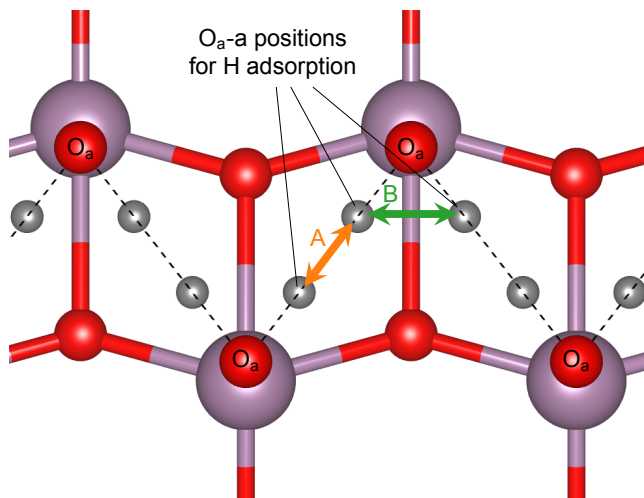


Figure 3. Zig-zag chain of O_a atoms in the intrabilayer region of α - MoO_3 . Gray spheres represent the O_a -a positions potentially occupied by H atoms, and paths A and B are diffusion paths of H atoms between the O_a -a positions investigated in the present study (cf. Section 3.4).

refer to as O_a -a. It is also possible that the H atom at the O_a site resides in the vdW gap and is directed to the O_t site of the next bilayer, a location we refer to as O_a -t. We can further consider the ideal H adsorption onto the O_a site within the reflection plane. In this case, H can be located inside and outside of the intrabilayer region, which we refer to as O_a -in and O_a -out, respectively.

1.4. Review on previous *ab initio* studies

While there are already several *ab initio* reports for the adsorption of an H atom on α - MoO_3 , the conclusions are often inconsistent among each other, both qualitatively and quantitatively. The most significant inconsistency regards the O site claimed to be the energetically most favorable for H to be adsorbed. Some studies [29, 35, 36] reported that the O_a site is energetically more favorable than the other O sites, consistent with powder neutron diffraction [16, 17] and nuclear magnetic resonance [18, 19] for bulk H_xMoO_3 with $x \leq 0.5$. Other *ab initio* reports [23, 24, 26, 28], in contrast, claimed that the O_t site is more favorable than the O_a site.

Table 1 summarizes the *ab initio* H adsorption energies on the MoO_3 surface reported previously. As mentioned in Section 1.1, from experiments H is expected to reside in the intrabilayer region and to be bonded to the O_a site for a relatively low H content of $x \leq 0.5$ in bulk H_xMoO_3 . This H location has, however, been rarely investigated in previous *ab initio* simulations, except for Chen *et al.* [35], which is likely one of the major reasons for the inconsistency among previous *ab initio* studies as well as with experiments. Another possible reason is the difference in the utilized exchange–correlation functional, i.e., specif-

ically, the difference between the local density approximation (LDA) and the generalized gradient approximation (GGA). This possibility was actually pointed out by Chen *et al.* [35], but no proof was given at that time.

The significant inconsistencies among previous *ab initio* studies prevent us from referring to the reported values with confidence. In the present study, we explain the inconsistencies with systematic calculations and provide reliable values of the H adsorption energies on MoO_3 .

2. COMPUTATIONAL DETAILS

2.1. H adsorption energy

The H adsorption energy may be computed with reference to either an H atom or an H_2 molecule. When we take an H atom as a reference, the adsorption energy for MoO_3 is computed as

$$\Delta E = \frac{1}{x} [E(\text{H}_x\text{MoO}_3) - (E(\text{MoO}_3) + xE(\text{H}))]. \quad (1)$$

When we take an H_2 molecule as a reference, the adsorption energy is computed as [37]

$$\Delta E = \frac{1}{x} \left[E(\text{H}_x\text{MoO}_3) - \left(E(\text{MoO}_3) + \frac{x}{2}E(\text{H}_2) \right) \right]. \quad (2)$$

In the present study, we computed the H adsorption energy with reference to an H atom, i.e., based on eq 1.

2.2. Electronic-structure calculations

The plane-wave basis projector augmented wave (PAW) method [38] was employed in the framework of density functional theory (DFT) as implemented in the VASP code [39–41]. The plane-wave cutoff energy was set to 500 eV, and the Methfessel–Paxton scheme [42] with a smearing width of 0.1 eV was employed for the sampling of the Brillouin zone. The 4s4p4d5s, 2s2p, and 1s orbitals of Mo, O, and H, respectively, were treated as the valence states. Total energies were minimized until they were converged to within 1×10^{-5} eV per simulation cell for each ionic step.

We considered several exchange–correlation functionals to investigate their impact on the results. LDA [43, 44] and GGA in the Perdew–Burke–Ernzerhof (PBE) form [45] were used in previous *ab initio* studies and therefore also considered in the present study. These functionals, however, do not consider the vdW interaction. While there are various approaches to include the vdW interaction in a DFT exchange–correlation functional, Peelaers and Van de Walle [46] reported that the semiempirical DFT-D2 functional proposed by Grimme [47] in combination with PBE shows reasonable agreements for lattice parameters with experimental values, at reasonable computational costs. We therefore considered the PBE-D2 functional. Furthermore, the strongly

Table 1. *Ab initio* H adsorption energies (in eV/(H atom)) on the MoO₃ surface as reported in previous studies. For the H adsorption at the O_a site, we have identified the H position from the visualizations provided in the articles. Note that the values referenced with respect to H₂ (eq 2) [27–29] are shifted to be consistent with the H-referenced values (eq 1) by the experimental H₂ atomization energy without zero-point energy (ZPE), 2.374 eV/(H atom) [34] (cf. Supporting Information).

	Year	Code	XC	O _t	O _s	O _a -out	O _a -a
Chen <i>et al.</i> [24]	1998	CASTEP	LDA	−3.39	−2.77	−3.13	N/A
Chen <i>et al.</i> [35]	2008	VASP	PW91	−2.45	−2.10	−2.67	−2.91
Mei <i>et al.</i> [28]	2011	VASP	PBE	−3.60	−2.70	−2.24	N/A
Yang <i>et al.</i> [27] ^a	2012	VASP	PBE	−2.78	N/A	N/A	N/A
Shetty <i>et al.</i> [29]	2017	CP2K	PBE	−2.70	−2.68	−3.24	N/A

^a Yang *et al.* [27] *a priori* assumed the O_t site as energetically the most favorable one for H with referring to Sha *et al.* [23], and the H adsorption energies for a single H atom at the O_s and the O_a sites were not given.

constrained and appropriately normed (SCAN) meta-GGA [48, 49] was considered, which accurately predicts electronic, thermodynamic, and electronic properties of various systems, even those with vdW interactions.

To determine the lattice parameters, bulk MoO₃ was computed employing a 16-atom unit cell. The Brillouin zone was sampled by a Γ -centered $2 \times 6 \times 6$ k -point mesh. Cell volume, cell shape, and internal atomic positions were optimized so that the forces on atoms and the stress components on the unit cell became less than 5×10^{-3} eV/Å and 2.5×10^{-4} eV/Å³, respectively. The structure optimization was repeated several times to be consistent with the given energy cutoff.

To model the MoO₃ surface, slab models with 1×1 , 2×2 and 3×3 expansions for the in-plane directions and with a vacuum region in the out-of-plane direction were used. Three different numbers of MoO₃ bilayers (1, 2 and 3) and three vacuum region thicknesses (12 Å, 14 Å and 16 Å) were considered. The Brillouin zones were sampled by k -point meshes consistent with the bulk calculations for the in-plane directions, and with one k -point for the out-of-plane direction. Internal atomic positions of the MoO₃ were optimized first without H with the same force convergence criterion as the bulk calculations and with keeping the cell volume and the cell shape consistent with the optimized bulk value.

For each optimized bulk and surface model of MoO₃, we put an H atom and reoptimized the internal atomic coordinates with fixed cell volume and cell shape. The force convergence criterion was set to 2×10^{-2} eV/Å. All the calculations including an H atom were performed considering spin polarization. In the bulk, we considered the nine H positions shown in Figure 2, while on the surface we considered seven H positions excluding O_a-t and O_t-a, which involve two bilayers. Transition states of the H diffusion were optimized using the improved dimer method [50].

3. RESULTS AND DISCUSSION

3.1. Structural parameters of bulk MoO₃

Table 2 shows the *ab initio* lattice parameters of bulk α -MoO₃ obtained in the present study.

For the in-plane lattice parameters b and c , all the exchange–correlation functionals except for LDA show a reasonable agreement with experiment with an error of only up to 1.5%. LDA underestimates b and c strongly, with an error up to 3.7%, demonstrating its overbinding nature [52–54].

For the out-of-plane lattice parameter a , PBE largely overestimates experiment by 15%, as also reported in previous studies [46, 55], clearly indicating the failure of PBE in describing the vdW interaction. LDA seems to show a good agreement with experiments, but as discussed frequently previously [56, 57], this is just due to error cancellation because LDA assigns an unphysically long range to exchange interactions and not because LDA captures the vdW interaction. In contrast, PBE-D2 and SCAN, both of which take the vdW interaction into account, predict a with an error of only up to 1.4%, consistent with previous studies [46, 55].

For the Mo–O bond lengths, in most cases all the investigated exchange–correlation functionals show good agreement with experimental values, but there are a few exceptions. Specifically, LDA shows an error of -7.6% for the longer Mo–O_a bond, and PBE and PBE-D2 show errors of $+5.9\%$ and $+3.5\%$, respectively, for the longer Mo–O_s bond. The SCAN functional does not show errors larger than 3% for any of the Mo–O bond lengths and thus best predicts the experimental structure, which is consistent with the results of Zhang *et al.* [55].

3.2. Surface energy of MoO₃

Figure 4 shows the *ab initio* surface energies of α -MoO₃ obtained in the present study.

The values are almost independent of the vacuum region thickness, indicating that even the smallest thickness (12 Å) would be enough to avoid bilayer interactions

Table 2. Lattice parameters and Mo–O bond lengths (in Å) of the bulk α -MoO₃ obtained in the present *ab initio* simulations. Experimental values of Kihlberg [51] are also shown for comparison.

	a	b	c	Mo–O _t	Mo–O _a	Mo–O _s	
LDA	13.575	3.678	3.816	1.675	1.766	2.079	2.341
PBE	15.988	3.691	3.936	1.680	1.760	2.200	1.947
PBE-D2	13.932	3.693	3.909	1.682	1.756	2.181	1.943
SCAN	14.044	3.681	3.907	1.673	1.745	2.185	2.380
Exp. [51]	13.855	3.6964	3.9628	1.671	1.734	2.251	2.332

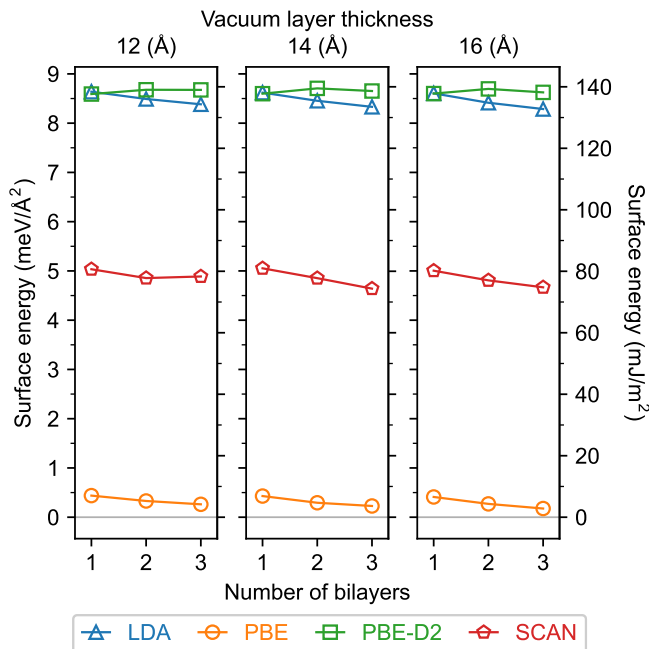


Figure 4. Surface energies of α -MoO₃ obtained in the present *ab initio* calculations.

between mirror images of the slab models. We hereafter focus on the results obtained using a vacuum layer thickness of 14 Å. The obtained surface energies are likewise almost independent of the number of bilayers, implying that the surface–surface interaction is marginal even for one bilayer.

PBE-D2 shows a surface energy of about $8.7 \text{ meV}/\text{\AA}^2$, while PBE shows a much smaller value of about $0.2 \text{ meV}/\text{\AA}^2$, indicating a very weak interaction between the bilayers due to the absence of the vdW interaction in PBE. SCAN shows a surface energy of about $4.6 \text{ meV}/\text{\AA}^2$, in between the values of PBE and PBE-D2. These values are in good agreement with a previous *ab initio* study [55]. LDA seems to show similar values to those of PBE-D2. As discussed in Section 3.1, however, by its nature LDA cannot correctly simulate the vdW interaction [56], and therefore the agreement should be attributed to a coincidence [57].

3.3. H adsorption energy in bulk MoO₃

Figure 5 shows the *ab initio* computed H adsorption energies in bulk α -MoO₃ for various computational conditions.

Among the investigated exchange–correlation functionals, LDA shows much lower adsorption energies than the other exchange–correlation functionals. In general, for various properties, PBE and SCAN show better agreements with experiments than LDA [48, 49]. The much lower H adsorption energies in LDA demonstrate the known overbinding nature of the LDA [52–54]. It should be however noted that the *relative* H adsorption energies among the investigated H positions predicted in LDA are still mostly similar to the other exchange–correlation functionals. PBE-D2 and SCAN, both of which are expected to be able to simulate the vdW interaction, show very similar trends, even quantitatively.

Except for LDA at $x = 0.25$, the O_a-a position is energetically the most favorable site for H regardless of the exchange–correlation functional and the H content. This is consistent with experiments for $x < 0.25$ [16–19], where H resides along the zig-zag chains of the O_a sites in the intrabilayer region.

At $x = 0.25$, LDA shows that the O_t site (O_t-t) is energetically slightly more stable than the O_a site (O_a-a). Specifically, for LDA, H adsorption energies are -3.32 eV and -3.28 eV at the O_t and the O_a sites, respectively, and therefore the O_t site is 0.04 eV more stable than the O_a site. For PBE, H adsorption energies are -2.47 eV and -2.49 eV at the O_t and the O_a sites, respectively, and therefore the O_a site is only 0.02 eV more stable than the O_t site. Although this small energy difference between the O_t and the O_a sites is in line with previous *ab initio* results by Sha *et al.* [23], it is contradictory to powder neutron diffraction [16, 17] and nuclear magnetic resonance [18, 19] for $x \leq 0.5$, which showed that H occupies the O_a site. For PBE-D2 and SCAN, in contrast to LDA and PBE, the O_a site is correctly predicted to be substantially more stable for H than the O_t site. Specifically, for PBE-D2, H adsorption energies are -2.44 eV and -2.66 eV at the O_t and the O_a sites, respectively, and therefore the O_a site is 0.22 eV more stable than the O_t site. For SCAN, H adsorption energies are -2.44 eV and -2.59 eV at the O_t and the O_a sites, respectively, and therefore the O_a site is 0.15 eV more stable than

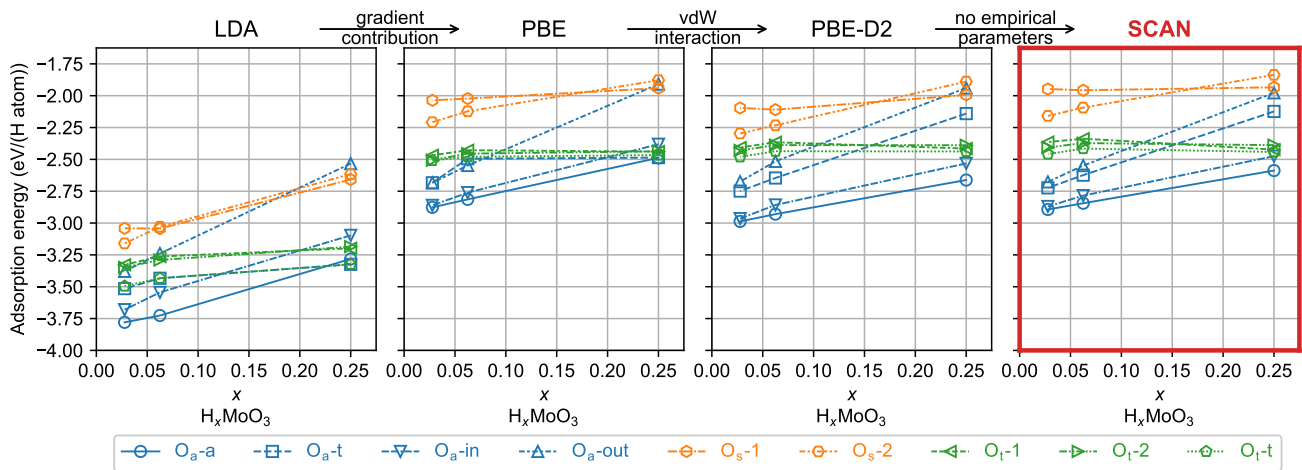


Figure 5. H adsorption energies in bulk MoO_3 with H as a reference (eq 1). The lines are guides for the eyes.

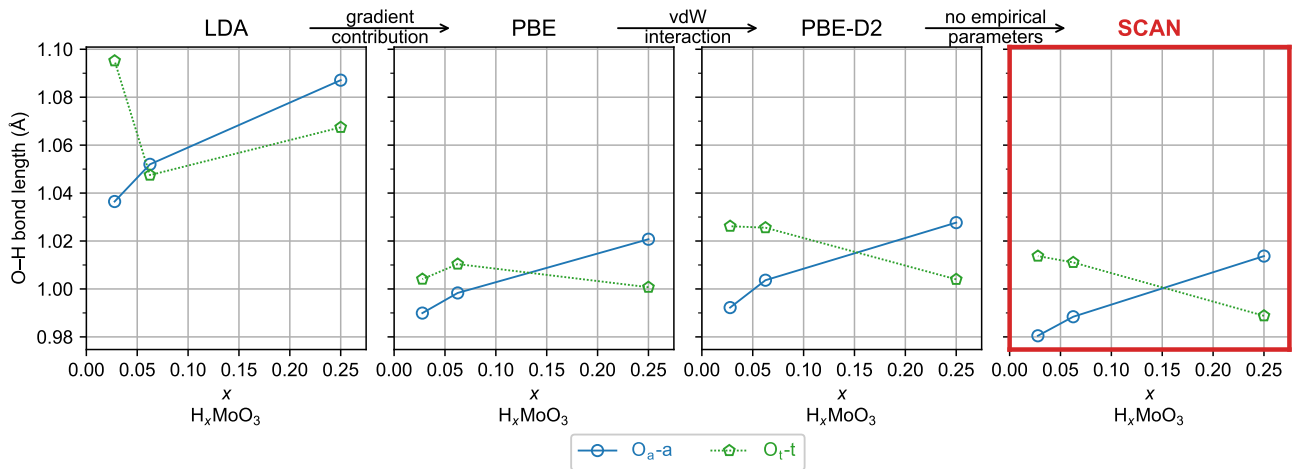


Figure 6. O–H bond lengths in bulk MoO_3 for the O_a -a and the O_t -t positions. The lines are guides for the eyes.

the O_t site. The poor agreement of LDA and PBE with the experimental observation can be probably ascribed to the lack of the consideration of the vdW interaction in these functionals. Particularly for PBE, since the interbilayer distance is largely overestimated (cf. Table 2), it may erroneously stabilize the O_t site, which faces the vdW region, as compared with the O_a site. These results clearly demonstrate the importance of exchange–correlation functionals which account for the vdW interaction to correctly predict the most stable H adsorption site.

For the dilute H concentration of $x \leq 0.0625$, where the H–H interaction is expected to be negligible, H substantially favors the O_a site rather than the O_t site, irrespective of the exchange–correlation functionals. When the H content increases, the H adsorption energy at the O_a site becomes less negative while the H adsorption energy at the O_t site is less sensitive against the H content. This implies that the O_t site would be energetically more stable than the O_a site at further higher H concentra-

tions, which is consistent with experimental observations for hydrogen molybdenum bronze. Specifically, at low H concentrations ($x \leq 0.5$) H is bound to the O_a site and located on the zig-zag chain in the intrabilayer region [16–19], while for higher H contents of $1.55 < x \leq 2$, powder neutron diffraction [20, 21] showed that H is bound to the O_t sites and resides in the interbilayer region.

Irrespective of the exchange–correlation functional as well as of the H content, the O_a -a position is the most favorable among the O_a sites, and the O_t -t position is the most favorable among the O_t sites. Figure 6 shows the O–H bond lengths for these two selected H positions. LDA shows substantially longer ($>1.03 \text{ \AA}$) O–H bond lengths compared with the other exchange–correlation functionals. In SCAN, when the H content increases, the O–H bond lengths become longer and shorter for the O_a -a and the O_t -t positions, respectively. This trend is correlated with the energetic stability of an H atom in Figure 5. That is, at the O_a -a position, H adsorption becomes less favorable with the increase of the H content, together

Table 3. H activation energies $\Delta^\ddagger E$ and O–H bond lengths for the transition states of the H diffusion paths A and B shown in [Figure 3](#) for bulk $\text{H}_{0.25}\text{MoO}_3$.

	$\Delta^\ddagger E$ (eV/(H atom))		O–H (Å)	
	A	B	A	B
LDA	0.011	0.185	1.231	1.007
PBE	0.116	0.107	1.248	0.993
PBE-D2	0.091	0.131	1.240	0.994
SCAN	0.146	0.113	1.236	0.984

with the elongation of the O–H bond lengths, and the opposite trend is found for the O_t -t position.

3.4. H activation energy in bulk MoO_3

Having verified that the O_a -a position is the most favorable for H in bulk α - MoO_3 , we now focus on the H activation energies in bulk α - MoO_3 for H diffusion between the O_a -a positions. Specifically, we consider the intralayer H diffusion paths A and B shown in [Figure 3](#). [Table 3](#) shows the *ab initio* computed H activation energies. Except for path A computed with LDA, the obtained H activation energies are 0.1–0.2 eV/(H atom) [58]. This is in good agreement with previous experimental values; the value by Slade *et al.* [59] (0.11 eV/(H atom) for $x = 0.36$) is almost in perfect agreement with our *ab initio* values, and the values of Ritter *et al.* [18] (0.31 eV/(H atom) for $x = 0.35$) and Ritter *et al.* [19] (0.28–0.31 eV/(H atom) for x in 0.2–0.35) are just slightly higher than our *ab initio* values.

While the O–H bond lengths are similar among the exchange–correlation functionals for both paths A and B, the trends of the H activation energies are different. In PBE and SCAN, path A shows lower H activation energies, while LDA and PBE-D2 show the opposite trend. From the known successes of the SCAN functional [48, 49] as well as the best geometrical agreement with experiments for bulk MoO_3 in the present study (cf. [Table 2](#)), we expect that SCAN provides more reliable results.

3.5. H adsorption energy on the MoO_3 surface

[Figure 7](#) shows the *ab initio* computed H adsorption energies on the MoO_3 surface for various computational conditions. The values are almost independent of the number of bilayers (top vs. bottom panels in each column) for all of the investigated exchange–correlation functionals and for all the H coverages, meaning that the impact of H is limited to within one bilayer.

Most of the trends are similar to the H adsorption in bulk MoO_3 . In particular, LDA gives much more negative H adsorption energies than the other functionals, which can be again ascribed to the overbinding nature of

LDA [52–54]. Previous *ab initio* studies using LDA [24] likewise showed significantly more negative H adsorption energies than GGA [27–29, 35], even taking the difference of the energy reference (eqs 1 and 2) into account (cf. Appendix), as shown in [Table 1](#).

The O_a -a site is energetically the most favorable among the investigated H positions for all the investigated exchange–correlation functionals and for all the investigated H coverages. As described in [Section 3.3](#), also in bulk MoO_3 the O_a -a site is the energetically most favorable one when $x \leq 0.0625$, which is supported by powder neutron diffraction [16, 17] and by nuclear magnetic resonance [18, 19] for bulk H_xMoO_3 with $x \leq 0.5$.

It should be pointed out that, if we consider only the O_a -out position and ignore the energetically more favorable O_a -a or O_a -in positions, as done in Refs. [24, 27–29], the O_t site (green in [Figure 7](#)) can be obtained as the energetically most preferable site in some cases. Particularly for LDA, regardless of the H coverage, the O_t site would be obtained as the energetically most stable site, if only the O_a -out position was considered for the O_a site, which is indeed the case in an early *ab initio* study using LDA [24, 60]. Our present results reveal that the previous erroneous results originate from the fact that 1) LDA was used and 2) the O_a -a H adsorption site was ignored, which is energetically more favorable than O_a -out.

Contrary to the present results ([Figure 7](#)), a previous *ab initio* study by Mei *et al.* [28] reported that even in PBE the O_t site is energetically the most favorable for H at a coverage of $\approx 1 \text{ nm}^{-2}$, although here and in Ref. [28] the same *ab initio* code (VASP) was used. Mei *et al.* [28] considered only the O_a -out position for H and did not consider the O_a -a and the O_a -in position [61]. According to our results, the O_a -a and the O_a -in positions are more than 0.2 eV lower in H adsorption energy than the O_a -out position in PBE and at an H coverage of $\approx 1 \text{ nm}^{-2}$, but this does not fully account for their results showing a much more stable O_t site. Other detailed computational conditions are also different between Mei *et al.* [28] and us. Specifically, we used a tighter force convergence criterion of 0.02 eV/Å for H-including calculations (0.05 eV/Å in Ref. [28]), a higher energy cutoff of 500 eV (400 eV in Ref. [28]), and a thicker vacuum region of 14 Å (12 Å in Ref. [28]). Furthermore, Mei *et al.* [28] fixed the in-plane lattice parameters to the experimental values for the bulk rather than relaxing them and also fixed the atoms in the bottom bilayers in their models including two bilayers which were not optimized. Such detailed differences are, however, not expected to lead to such a contradictory conclusion. We therefore attribute the contradiction to potential erroneous analyses in the previous research [28].

In [Figure 7](#), the H adsorption energy at the O_a -a site becomes less negative when the H coverage becomes higher, similarly to the H adsorption in bulk MoO_3 (cf. [Figure 5](#)), which should be ascribed to the H–H repulsion. This means that, under the assumption that all the H atoms are adsorbed on the O atoms in the same

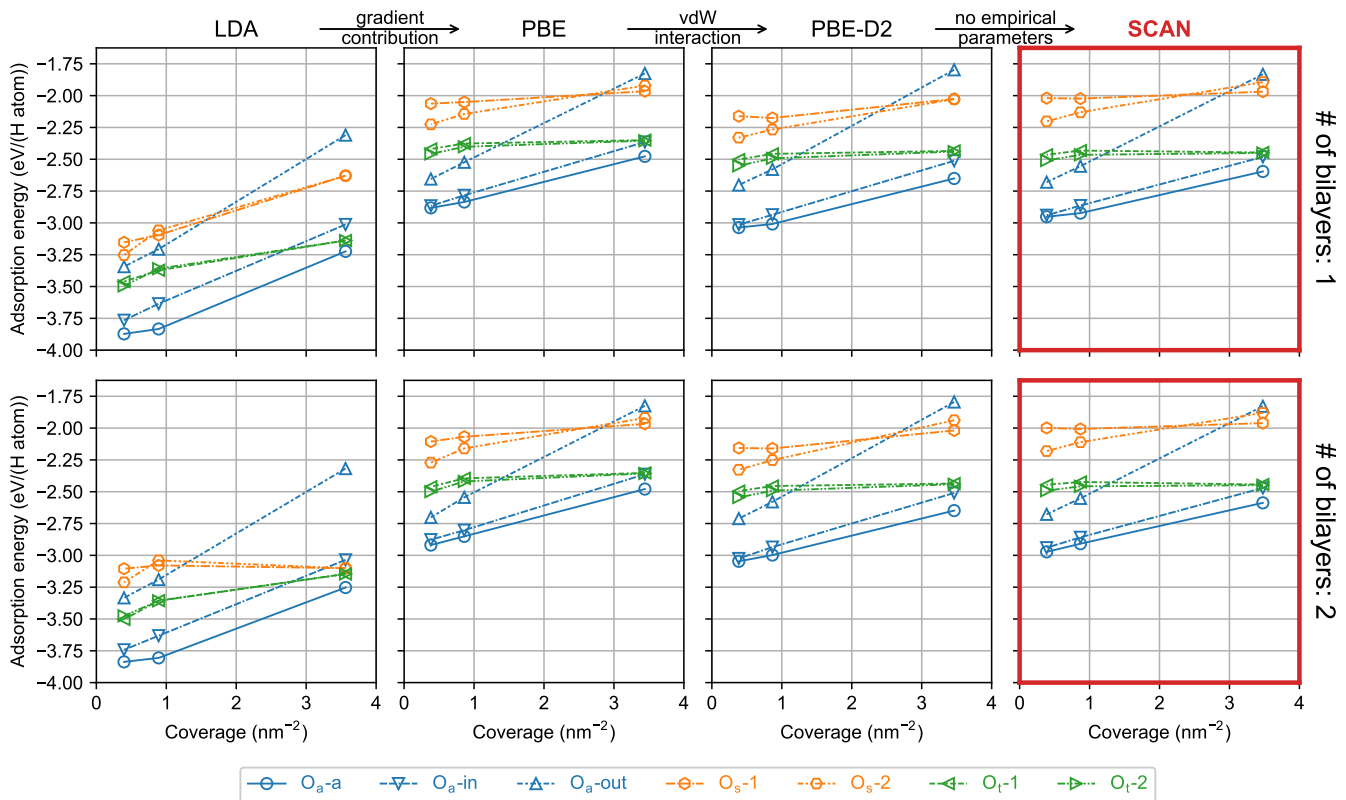


Figure 7. H adsorption energies on the MoO_3 surface with H as a reference (eq 1). The lines are guides for the eyes.

way, H adsorption becomes energetically less preferable when the amount of H increases.

4. CONCLUSIONS

In the present study, we have performed detailed investigations of the H adsorption on $\alpha\text{-MoO}_3$ based on systematic *ab initio* calculations and critical analysis of the existing literature. Both in the bulk and on the surface of MoO_3 , H prefers to bind to O at the asymmetric site (O_a) and to reside in the intrabilayer region along the zigzag chains consisting of the O_a sites (cf. Figure 3), which is supported by powder neutron diffraction [16, 17] and by nuclear magnetic resonance [18, 19] for bulk H_xMoO_3 with $x \leq 0.5$. Previous contradictory *ab initio* results are ascribed to the use of exchange–correlation functionals that either do not take the vdW interaction into account, such as the LDA and the PBE functionals, or to the neglect of H adsorption at the O_a site *in the intrabilayer region*. Particularly for bulk MoO_3 , the lack of the vdW interaction in the exchange–correlation functionals is critical, because the distances between the bilayers are overestimated and thus the strength of the H bonding to the O atom at the terminal site (O_t) is predicted as too strong. It is clearly advisable to use an exchange–correlation functional that takes the vdW interaction into account, such as the SCAN meta-GGA functional. In-

deed, the SCAN functional offers an H activation energy of 0.11–0.15 eV/(H atom), in good agreement with experimental values. For dilute H content, i.e., $x = 0.0625$ in bulk H_xMoO_3 , the H adsorption energy is predicted as -2.89 eV/(H atom) at the O_a site in the intrabilayer region using the SCAN functional. Table 4 summarizes the H adsorption energies obtained with SCAN.

ASSOCIATED CONTENT

Supporting Information

The Supporting Information contains the results of H_2 atomization energies and zero-point energies.

ACKNOWLEDGMENTS

This project has received funding from the European Research Council (ERC) under the European Union’s Horizon 2020 research and innovation programme (grant agreement No 865855). The authors also acknowledge support by the state of Baden-Württemberg through bwHPC and the German Research Foundation (DFG) through grant no INST 40/467-1 FUGG (JUSTUS cluster). B.G. acknowledges the support by the Stuttgart

Table 4. H adsorption energies obtained with SCAN as a function of the in-plane supercell expansion. Corresponding H coverages per bilayer (in nm⁻²) are also shown.

Coverage # of bilayers		O _a -a	O _a -in	O _a -out	O _a -t	O _s -1	O _s -2	O _t -1	O _t -2	O _t -t	
1 × 1	3.477	1	-2.596	-2.481	-1.832	N/A	-1.969	-1.894	-2.447	-2.451	N/A
		2	-2.587	-2.470	-1.828	N/A	-1.961	-1.881	-2.444	-2.449	N/A
		bulk	-2.588	-2.475	-1.977	-2.124	-1.934	-1.837	-2.423	-2.388	-2.442
2 × 2	0.869	1	-2.923	-2.864	-2.555	N/A	-2.023	-2.131	-2.432	-2.465	N/A
		2	-2.909	-2.858	-2.552	N/A	-2.007	-2.110	-2.423	-2.458	N/A
		bulk	-2.844	-2.785	-2.549	-2.624	-1.957	-2.093	-2.337	-2.372	-2.415
3 × 3	0.386	1	-2.952	-2.940	-2.680	N/A	-2.020	-2.202	-2.464	-2.509	N/A
		2	-2.973	-2.940	-2.677	N/A	-1.999	-2.181	-2.445	-2.492	N/A
		bulk	-2.893	-2.870	-2.676	-2.724	-1.948	-2.159	-2.364	-2.406	-2.458

Center for Simulation Science (SimTech). D.P.E. grate-

fully acknowledges the Deutsche Forschungsgemeinschaft (project number 444948747) for funding.

- [1] D. O. Scanlon, G. W. Watson, D. J. Payne, G. R. Atkinson, R. G. Egdell, and D. S. L. Law, Theoretical and experimental study of the electronic structures of MoO₃ and MoO₂, *J. Phys. Chem. C* **114**, 4636 (2010).
- [2] T. Tsumura, Lithium insertion/extraction reaction on crystalline MoO₃, *Solid State Ionics* **104**, 183 (1997).
- [3] W. Li, F. Cheng, Z. Tao, and J. Chen, Vapor-transportation preparation and reversible lithium intercalation/deintercalation of α -MoO₃ microrods, *J. Phys. Chem. B* **110**, 119 (2006).
- [4] H. C. Zeng, Chemical etching of molybdenum trioxide: a new tailor-made synthesis of MoO₃ catalysts, *Inorg. Chem.* **37**, 1967 (1998).
- [5] F. Uchijima, T. Takagi, H. Itoh, T. Matsuda, and N. Takahashi, Catalytic properties of h₂-reduced MoO₃ with noble metal for the conversions of heptane and propan-2-ol, *Phys. Chem. Chem. Phys.* **2**, 1077 (2000).
- [6] T. Prasomsri, T. Nimmanwudipong, and Y. Román-Leshkov, Effective hydrodeoxygenation of biomass-derived oxygenates into unsaturated hydrocarbons by MoO₃ using low H₂ pressures, *Energy Environ. Sci.* **6**, 1732 (2013).
- [7] C. Ranga, R. Lødeng, V. I. Alexiadis, T. Rajkhowa, H. Bjørkan, S. Chytil, I. H. Svenum, J. Walmsley, C. Detavernier, H. Poelman, P. V. D. Voort, and J. W. Thybaut, Effect of composition and preparation of supported MoO₃ catalysts for anisole hydrodeoxygenation, *Chem. Eng. J.* **335**, 120 (2018).
- [8] Y. A. Yang, Y. W. Cao, B. H. Loo, and J. N. Yao, Microstructures of electrochromic MoO₃ thin films colored by injection of different cations, *J. Phys. Chem. B* **102**, 9392 (1998).
- [9] J. N. Yao, K. Hashimoto, and A. Fujishima, Photochromism induced in an electrolytically pretreated MoO₃ thin film by visible light, *Nature* **355**, 624 (1992).
- [10] D. Xiang, C. Han, J. Zhang, and W. Chen, Gap states assisted MoO₃ nanobelt photodetector with wide spectrum response, *Sci. Rep.* **4**, 10.1038/srep04891 (2014).
- [11] E. Comini, L. Yubao, Y. Brando, and G. Sberveglieri, Gas sensing properties of MoO₃ nanorods to CO and CH₃OH, *Chem. Phys. Lett.* **407**, 368 (2005).
- [12] M. Ferroni, V. Guidi, G. Martinelli, M. Sacerdoti, P. Nelli, and G. Sberveglieri, MoO₃-based sputtered thin films for fast NO₂ detection, *Sens. Actuators B Chem.* **48**, 285 (1998).
- [13] H.-S. Kim, J. B. Cook, H. Lin, J. S. Ko, S. H. Tolbert, V. Ozolins, and B. Dunn, Oxygen vacancies enhance pseudocapacitive charge storage properties of MoO_{3-x}, *Nat. Mater.* **16**, 454 (2016).
- [14] Y. Li and R. T. Yang, Hydrogen storage in metal-organic frameworks by bridged hydrogen spillover, *J. Am. Chem. Soc.* **128**, 8136 (2006).
- [15] Y. Li and R. T. Yang, Hydrogen storage in low silica type X zeolites, *J. Phys. Chem. B* **110**, 17175 (2006).
- [16] F. A. Schröder and H. Weitzel, Beiträge zur chemie von molybdän und wolfram. XXI. Mo₄O₁₀(OH)₂ - eine verbindung mit nicht ganzzahliger stöchiometrie: MoO_{3-x}(OH)_x, *Z. Anorg. Allg. Chem.* **435**, 247 (1977).
- [17] P. Dickens, J. Birtill, and C. Wright, Elastic and inelastic neutron studies of hydrogen molybdenum bronzes, *J. Solid State Chem.* **28**, 185 (1979).
- [18] C. Ritter, W. Müller-Warmuth, H. W. Spiess, and R. Schöllhorn, Quasi-one-dimensional behaviour of hydrogen in H_{0.35}MoO₃ and H_{0.33}WO₃ as revealed by proton NMR, *Ber. Bunsenges. Phys. Chem.* **86**, 1101 (1982).
- [19] C. Ritter, W. Müller-Warmuth, and R. Schöllhorn, Structure and motion of hydrogen in molybdenum bronzes H_xMoO₃ as studied by nuclear magnetic resonance, *J. Chem. Phys.* **83**, 6130 (1985).
- [20] P. G. Dickens, A. T. Short, and S. Crouch-Baker, The crystal structure of D_{1.7}MoO₃ by powder neutron diffraction, *Solid State Ionics* **28-30**, 1294 (1988).
- [21] M. Anne, D. Fruchart, S. Derdour, and D. Tinet, Structure of D_{1.65}MoO₃ by neutron diffraction, *J. Phys. France* **49**, 505 (1988).
- [22] B. Braïda, S. Adams, and E. Canadell, Concerning the structure of hydrogen molybdenum bronze phase III. a combined theoretical-experimental study, *Chem. Mater.* **17**, 5957 (2005).

- [23] X. Sha, L. Chen, A. C. Cooper, G. P. Pez, and H. Cheng, Hydrogen absorption and diffusion in bulk α -MoO₃, *J. Phys. Chem. C* **113**, 11399 (2009).
- [24] M. Chen, U. V. Waghmare, C. M. Friend, and E. Kaxiras, A density functional study of clean and hydrogen-covered α -MoO₃(010): Electronic structure and surface relaxation, *J. Chem. Phys.* **109**, 6854 (1998).
- [25] M. Chen, C. M. Friend, and E. Kaxiras, A density functional theory study of site-specific methyl reaction on MoO₃(010): The effects of methyl coverage, *J. Chem. Phys.* **112**, 9617 (2000).
- [26] M. Chen, C. M. Friend, and E. Kaxiras, The chemical nature of surface point defects on MoO₃(010): adsorption of hydrogen and methyl, *J. Am. Chem. Soc.* **123**, 2224 (2001).
- [27] M. Yang, B. Han, and H. Cheng, First-principles study of hydrogenation of ethylene on a H_xMoO₃(010) surface, *J. Phys. Chem. C* **116**, 24630 (2012).
- [28] D. Mei, A. M. Karim, and Y. Wang, Density functional theory study of acetaldehyde hydrodeoxygenation on MoO₃, *J. Phys. Chem. C* **115**, 8155 (2011).
- [29] M. Shetty, B. Buesser, Y. Román-Leshkov, and W. H. Green, Computational investigation on hydrodeoxygenation (HDO) of acetone to propylene on α -MoO₃(010) surface, *J. Phys. Chem. C* **121**, 17848 (2017).
- [30] Q. Pan, L. Huang, Z. Li, J. Han, N. Zhao, Y. Xie, X. Li, M. Liu, X. Wang, and J.-M. Liu, A first-principles study on the hydrogenation of acetone on H_xMoO₃ surface, *Int. J. Hydrog. Energy* **44**, 10443 (2019).
- [31] M. Rellán-Piñeiro and N. López, One oxygen vacancy, two charge states: Characterization of reduced α -MoO₃(010) through theoretical methods, *J. Phys. Chem. Lett.* **9**, 2568 (2018).
- [32] K. Momma and F. Izumi, *VESTA3* for three-dimensional visualization of crystal, volumetric and morphology data, *J. Appl. Crystallogr.* **44**, 1272 (2011).
- [33] M. I. Aroyo, ed., *International Tables for Crystallography Volume A: Space-group symmetry*, 6th ed. (International Union of Crystallography, 2016).
- [34] K. K. Irikura, Experimental vibrational zero-point energies: Diatomic molecules, *J. Phys. Chem. Ref. Data* **36**, 389 (2007); Erratum: Experimental vibrational zero-point energies: Diatomic molecules [J. Phys. Chem. Ref. Data 36, 389–397 (2007)], *J. Phys. Chem. Ref. Data* **38**, 749 (2009).
- [35] L. Chen, A. C. Cooper, G. P. Pez, and H. Cheng, On the mechanisms of hydrogen spillover in MoO₃, *J. Phys. Chem. C* **112**, 1755 (2008).
- [36] F. Haque, A. Zavabeti, B. Y. Zhang, R. S. Datta, Y. Yin, Z. Yi, Y. Wang, N. Mahmood, N. Pillai, N. Syed, H. Khan, A. Jannat, N. Wang, N. Medhekar, K. Kalantar-zadeh, and J. Z. Ou, Ordered intracrystalline pores in planar molybdenum oxide for enhanced alkaline hydrogen evolution, *J. Mater. Chem. A* **7**, 257 (2019).
- [37] Some previous studies [27, 29] used eq 2 but with a factor of two, meaning that they considered the adsorption of an H₂ molecule rather than an H atom.
- [38] P. E. Blöchl, Projector augmented-wave method, *Phys. Rev. B* **50**, 17953 (1994).
- [39] G. Kresse, *Ab initio* molecular dynamics for liquid metals, *J. Non-Cryst. Solids* **192–193**, 222 (1995).
- [40] G. Kresse and J. Furthmüller, Efficiency of *ab-initio* total energy calculations for metals and semiconductors using a plane-wave basis set, *Comput. Mater. Sci.* **6**, 15 (1996).
- [41] G. Kresse and D. Joubert, From ultrasoft pseudopotentials to the projector augmented-wave method, *Phys. Rev. B* **59**, 1758 (1999).
- [42] M. Methfessel and A. T. Paxton, High-precision sampling for Brillouin-zone integration in metals, *Phys. Rev. B* **40**, 3616 (1989).
- [43] D. M. Ceperley and B. J. Alder, Ground state of the electron gas by a stochastic method, *Phys. Rev. Lett.* **45**, 566 (1980).
- [44] J. P. Perdew and A. Zunger, Self-interaction correction to density-functional approximations for many-electron systems, *Phys. Rev. B* **23**, 5048 (1981).
- [45] J. P. Perdew, K. Burke, and M. Ernzerhof, Generalized gradient approximation made simple, *Phys. Rev. Lett.* **77**, 3865 (1996).
- [46] H. Peelaers and C. G. Van de Walle, First-principles study of van der Waals interactions in MoS₂ and MoO₃, *J. Phys.: Condens. Matter* **26**, 305502 (2014).
- [47] S. Grimme, Semiempirical GGA-type density functional constructed with a long-range dispersion correction, *J. Comput. Chem.* **27**, 1787 (2006).
- [48] J. Sun, A. Ruzsinszky, and J. Perdew, Strongly constrained and appropriately normed semilocal density functional, *Phys. Rev. Lett.* **115**, 036402 (2015).
- [49] J. Sun, R. C. Remsing, Y. Zhang, Z. Sun, A. Ruzsinszky, H. Peng, Z. Yang, A. Paul, U. Waghmare, X. Wu, M. L. Klein, and J. P. Perdew, Accurate first-principles structures and energies of diversely bonded systems from an efficient density functional, *Nat. Chem.* **8**, 831 (2016).
- [50] A. Heyden, A. T. Bell, and F. J. Keil, Efficient methods for finding transition states in chemical reactions: Comparison of improved dimer method and partitioned rational function optimization method, *J. Chem. Phys.* **123**, 224101 (2005).
- [51] L. Kihlberg, Least squares refinement of crystal structure of molybdenum trioxide, *Ark. Kemi.* **21**, 357 (1963).
- [52] P. Haas, F. Tran, and P. Blaha, Calculation of the lattice constant of solids with semilocal functionals, *Phys. Rev. B* **79**, 085104 (2009); Erratum: Calculation of the lattice constant of solids with semilocal functionals [Phys. Rev. B 79, 085104 (2009)], *Phys. Rev. B* **79**, 209902 (2009).
- [53] B. Grabowski, T. Hickel, and J. Neugebauer, *Ab initio* study of the thermodynamic properties of nonmagnetic elementary fcc metals: Exchange-correlation-related error bars and chemical trends, *Phys. Rev. B* **76**, 024309 (2007).
- [54] T. Hickel, B. Grabowski, F. Körmann, and J. Neugebauer, Advancing density functional theory to finite temperatures: methods and applications in steel design, *J. Phys.: Condens. Matter* **24**, 053202 (2011).
- [55] T. Zhang, X. Yang, and Q. Ge, Surface chemistry and reactivity of α -MoO₃ toward methane: A SCAN-functional based DFT study, *J. Chem. Phys.* **151**, 044708 (2019).
- [56] J. Harris, Simplified method for calculating the energy of weakly interacting fragments, *Phys. Rev. B* **31**, 1770 (1985).
- [57] T. Björkman, A. Gulans, A. V. Krashennnikov, and R. M. Nieminen, Are we van der Waals ready?, *J. Phys.: Condens. Matter* **24**, 424218 (2012).
- [58] Chen *et al.* [35] obtained a bit higher H activation energy of 0.35 eV/(H atom) for path A using the PW91 functional, but since lattice parameters they employed are unclear, a fair comparison is not possible.

- [59] R. Slade, T. Halstead, and P. Dickens, NMR study of hydrogen molybdenum bronzes: $\text{H}_{1.71}\text{MoO}_3$ and $\text{H}_{0.36}\text{MoO}_3$, *J. Solid State Chem.* **34**, 183 (1980).
- [60] In the caption of Figure 4 in Chen *et al.* [26], the symmetric and the asymmetric oxygen sites are erroneously referred to.
- [61] See Figure 2(b) in Mei *et al.* [28]. Note that they notate the asymmetric site (O_a in the notation of the present paper) as O_b .

Supporting Information

Comprehensive understanding of H adsorption on MoO₃ from systematic *ab initio* simulations

Yuji Ikeda,^{1,*} Deven Estes,² and Blazej Grabowski¹

¹*Institute for Materials Science, University of Stuttgart, Pfaffenwaldring 55, 70569 Stuttgart, Germany*

²*Institute of Technical Chemistry, University of Stuttgart, Pfaffenwaldring 55, 70569, Stuttgart, Germany*

Appendix: H₂ atomization energy

When comparing the H adsorption energies reported in previous *ab initio* studies (Table 1 in the main text), one of the issues is the difference of the definition of the H adsorption energy, i.e., whether we set an H atom (eq 1 in the main text) or an H₂ molecule (eq 2 in the main text) as a reference. For a fair comparison, we have corrected the values referring to H₂ [S1–S3] to refer to H by utilizing the experimental energy difference between H₂ and 2H extracted below. We have also compared the *ab initio* obtained values with the experimental ones to check the consistency.

The *ab initio* calculations of H and H₂ were performed in a 20 Å × 20 Å × 20 Å simulation cell, and only the Γ point was used to sample the Brillouin zone. The atomic distance of H₂ was optimized so that the forces on atoms are less than 5×10^{-3} eV/Å. For H, spin-polarization was considered. Other relevant computational conditions were the same as those described in Section 2.2 in the main text. The zero-point energy (ZPE) of H₂ was evaluated within the harmonic approximation based on the finite displacement method with the displacement of 0.01 Å.

Table S1 summarizes the such computed *ab initio* bond lengths, ZPEs, and atomization energies, as well as experimental values extracted from literature [S4–S6]. For all the investigated exchange–correlation functionals, the computed values are found to be in reasonable agreement with experiment. It is therefore safe to use the experimental value of the atomization energy to correct the values for a qualitative comparison in Table 1 in the main text. Since the *ab initio* studies referred to in Table 1 in the main text did not account for the contribution of lattice vibrations, it is fair to correct the values in Table 1 in the main text with the value *without* ZPE. We therefore took the experimental atomization energy of H₂ without ZPE, 4.748 eV/(H atom), and corrected the values in Refs. [S1–S3] in Table 1 in the main text, which reference to H₂ (eq 2 in the main text), by 2.374 eV/(H atom).

Table S1. Bond lengths (in Å), ZPEs (in eV/molecule), and atomization energies $\Delta_{\text{at}}E$ (in eV/molecule) of H₂. Note that PBE-D2 shows essentially the same results as PBE.

	Bond length	ZPE	$\Delta_{\text{at}}E$	
			w/o ZPE	w/ ZPE
LDA	0.766	0.258	4.906	4.648
PBE	0.750	0.267	4.537	4.270
PBE-D2	0.750	0.267	4.537	4.270
SCAN	0.741	0.275	4.665	4.390
Exp.	0.741 44 ^a	0.270 ^b	4.748 ^{b,c}	4.478 ^c

^a Ref. [S4].

^b Ref. [S6].

^c Ref. [S5].

* yuji.ikeda@imw.uni-stuttgart.de

-
- [S1] D. Mei, A. M. Karim, and Y. Wang, Density functional theory study of acetaldehyde hydrodeoxygenation on MoO₃, *J. Phys. Chem. C* **115**, 8155 (2011).
- [S2] M. Yang, B. Han, and H. Cheng, First-principles study of hydrogenation of ethylene on a H_xMoO₃(010) surface, *J. Phys. Chem. C* **116**, 24630 (2012).
- [S3] M. Shetty, B. Buesser, Y. Román-Leshkov, and W. H. Green, Computational investigation on hydrodeoxygenation (HDO) of acetone to propylene on α -MoO₃(010) surface, *J. Phys. Chem. C* **121**, 17848 (2017).
- [S4] K. P. Huber and G. Herzberg, *Molecular Spectra and Molecular Structure* (Springer, New York, 1979).
- [S5] M. W. Chase, Jr., *JANAF Thermochemical Tables*, 4th ed. (American Institute of Physics, New York, 1998).
- [S6] K. K. Irikura, Experimental vibrational zero-point energies: Diatomic molecules, *J. Phys. Chem. Ref. Data* **36**, 389 (2007).